Stress Intensity Factor for a Crack Emanating from a Corner of a Square Hole

by

Mohamad Amirul bin Mohamad Yusuf

Dissertation submitted in partial fulfilment of
the requirements for the
Bachelor of Engineering (Hons)
(Mechanical Engineering)

DECEMBER 2010

Universiti Teknologi PETRONAS
Bandar Seri Iskandar
31750 Tronoh
Perak Darul Ridzuan

CERTIFICATION OF APPROVAL

Stress Intensity Factor for a Crack Emanating from a Corner of a Square Hole

by

Mohamad Amirul bin Mohamad Yusuf

A project dissertation submitted to the
Mechanical Engineering Programme
Universiti Teknologi PETRONAS
in partial fulfilment of the requirements for the
Bachelor of Engineering (Hons)
(Mechanical Engineering)

DECEMBER 2010

Approved by

____

(Dr Saravanan Karuppanan)

UNIVERSITI TEKNOLOGI PETRONAS
TRONOH, PERAK
December 2010

CERTIFICATION OF ORIGINALITY

This is to verify that I am responsible for the work submitted in this project, that the original work is my own except as specified in the references and acknowledgements, and that the original work contained herein have not been undertaken or done by unspecified sources or person

____

MOHAMAD AMIRUL B MOHAMAD YUSUF

ABSTRACT

This project is about the assessment of stress intensity factor for a crack emanating from a corner of a square hole. In this project, finite element analysis (FEA) software package, ANSYS will be used to determine the stress intensity factor. The results from the finite element method by ANSYS will be compared to the semi-analytical solution that is developed by N. Hasebe and M. Ueda [1]. The analysis will be carried out using linear isotropic and elastic approach in plane strain condition as described in the linear elastic fracture mechanics [2].

The project is focused on the determination of the geometry factor, F of stress intensity factor, K for different models that is varied in terms of the square angle and also the crack length while the square length is set to be constant. By using ANSYS software, the models will be assessed thoroughly and the stress intensity factor for each model is determined. Then, the results will be compared to the semi-analytical solution provided in the literature [1].

The model is subjected to 2 modes of loading which are Mode I loading (uniform tension in x and y-axis) and Mode II loading (pure shear acting along the surface of the model).

For Mode I loading (uniform tension in x-axis), it can be concluded that as the crack length, c is increasing, the geometry factor, F will decrease. For Mode I loading (uniform tension in y-axis), it can be concluded that as the crack length, c is increasing, the geometry factor, F will increase. For Mode II loading, it can be concluded that as the crack length, c is increasing, the geometry factor, F will increase. Generally the finite element results agree well with the semi-analytical solutions.

ACKNOWLEDGEMENTS

The author wishes to take the opportunity to express his utmost gratitude to the individual that have taken the time and effort to assist the author in completing the project. Without the cooperation of these individuals, no doubt the author would have faced some minor complications throughout the course.

First and foremost the author's utmost gratitude goes to the author supervisor, Dr Saravanan Karuppanan. Without his guidance and patience, the author would not have succeeded to complete the project.

To the graduate assistant in Mechanical Engineering Department Mr Julendra Ariatedja, thank you for assisting the author in completing his project.

To all individuals that has helped the author in any way, but whose name is not mentioned here, the author thank you all

Table of Contents

List of Figures

List of Tables

CHAPTER 1
INTRODUCTION

1.1. Background

In common cases of engineering failure, engineers found that most of the failure began with cracks. For example, growth of cracks in pressure vessels due to crack propagation could cause a fatal explosion. Engineering failure analysis will be conducted to investigate the fallen structures or equipment and most of it is caused by cracks. A crack is defined as a narrow opening between two parts of something which has split or been broken. Growth of these cracks may be caused by material defects, discontinuities in assembly and/or design, harsh environments and damages in service.

The stress intensity factor, K defines the magnitude of the local stresses or stress distribution near the crack tip. This quantity is dependant of the loading applied to the sample, crack size, crack shape, and geometric boundaries of a sample. Engineers predict the stress state near the crack tip by using stress intensity factor in order to compare it with the fracture toughness, K_C property of the material. Fracture toughness is a property which describes the ability of a material containing a crack to resist fracture. A sample will fracture if $K > Kc$.

It is important to determine the stress intensity factor for a specific geometry and loading involved in order to assess the safety level for a solid. Thus, engineers can determine acceptable stress levels, establish acceptable defect size and verify material properties for certain working condition for a specific structural design.

1.2. Problem Statement

Assessing stress intensity factor, K is important in determination of stress distribution near the crack tip. It is vital in order to predict the crack propagation based on material fracture toughness. However, the practice to determined stress intensity factor experimentally is time consuming and expensive.

1.3. Objective

The objectives of this project are:

1. To model and determine the stress intensity factor for a crack emanating from a corner of a square hole by using finite element method.
2. To compare the finite element method results with those results obtained semi-analytically.

1.4. Scope of Study

The scope of work of this project is to model and determine the stress intensity factors for several models by using ANSYS. For each model, different modes of loading will be considered, and the results will be verified by comparing them with the semi-analytical results. The models will be subjected to 2 modes of loading; tensions in *x* and *y*-axis and pure shear. 4 types of square angle; 30°, 60°, 90° and 120° will be studied. All results obtained by ANSYS will be compared with the solution in the literature.

CHAPTER 2

LITERATURE REVIEW and/or THEORY

2.1. Stress Intensity Factor, *K*

Stress intensity factor, K is used to predict the stress distribution near the crack tip caused by an applied load or residual stress. Figure 2.1(a) shows an infinite plate that experience uniform tension, σ with a through crack present in the plate. Figure 2.1(b) shows the normal and shear stress components of an element around the crack tip of the plate. The crack tip creates stress singularity and this makes the stress concentration approach to find the stress state around the crack tip inappropriate. Therefore, stress intensity factor is introduced as in Equation 1 to represent the stress distribution at the crack tip.

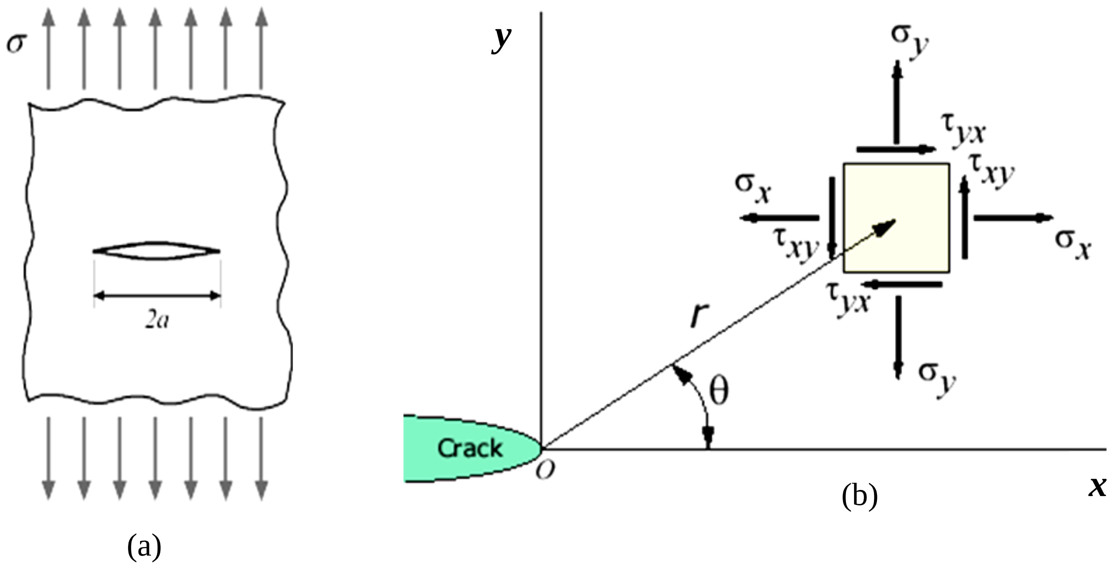

Figure 2.1: (a) A Plate with Uniform Tension in *y*-axis (b) Normal and Shear Stress Components of an Element around the Crack Tip in a Plate

$$\lim_{r\to 0} \sigma = \frac{K}{\sqrt{2\pi r}} F(\theta) \quad (1)$$

Thus, the stress intensity factor is commonly expressed in terms of the applied stresses, σ at $r \rightarrow 0$ and $\theta \rightarrow 0$ which is simplified to

$$K = F\sigma\sqrt{\pi a} \tag{2}$$

where K is the stress intensity factor, F is the geometry factor, σ is the applied stress and a is the crack length. The value and rate of change of the stress intensity factor directly influences the rate of crack growth in a component. The stress intensity factor does help to provide an accurate understanding of stress levels in the crack tip region, but assumes a purely elastic situation. The accuracy is reduced as the location approaches the actual crack tip where local plastic deformation occurs. The stress intensity factor is also more accurate when evaluating brittle materials as opposed to ductile materials that deform significantly prior to failure.

2.2. Linear Elastic Fracture Mechanics

Linear Elastic Fracture Mechanics (LEFM) has become a practical analytical tool for studying structural fracture where the inelastic deformation surrounding a crack tip is small. In applying LEFM analysis, several assumption have been made; material is linearly isotropic and elastic, crack has been initiated, crack has started to propagate, plastic zone near crack is small and point of analysis are near the crack tip. Based on the first assumption that the material is linear isotropic and elastic the stress field near the crack tip is calculated using the theory of elasticity.

In Linear Elastic Fracture Mechanics, most formulas are derived for either plane stresses or plane strains conditions, associated with the three basic modes of loadings on a cracked body: opening, sliding, and tearing [7].

LEFM is valid only when the inelastic deformation is small compared to the size of the crack (small-scale yielding). If large zones of plastic deformation develop before the crack grows, Elastic Plastic Fracture Mechanics (EPFM) must be used [7].

2.3. Fracture Toughness

The critical stress intensity factor, K_C can also be referred as fracture toughness and this material property is measured under precisely defined procedures prescribed by the American Society for Testing and Material (ASTM) standard E399.

When the combination of nominal stress and crack size attains a value such that the stress intensity factor, K reaches a critical magnitude K_C, unstable crack propagation occurs. Thus, assessing stress intensity factor properties of materials is crucial in order to prevent failures.

2.4. Stress Intensity Factor for a Crack Emanating From a Corner of a Square Hole

The solution of the geometry with a crack emanating from a corner of a square hole as in Figure 2.2 is obtained through conformal mapping based on Muskhelishvili's method according to Y. Murakami [1] where $\alpha\pi$ is the square angle, b is the square length and c is the crack length.

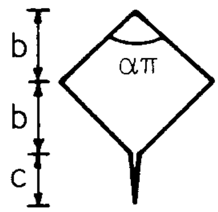

Figure 2.2: A Crack Emanating from the Corner of a Square Hole

Generally there are three loading modes to describe different crack surface displacement which are opening or tensile mode, sliding or in-plane shear mode and also tearing or anti-plane shear mode. However, in this project only two modes are considered; Mode I uniform tension in the direction of x or y – axis and Mode II pure shear acting along the surface of the square hole.

2.4.1. Uniform Tension in the Direction of *x* or *y* – axis (Mode I Loading)

Figure 2.3 below shows the geometry of a crack emanating from a corner of a square hole subject to Mode I loading [1].

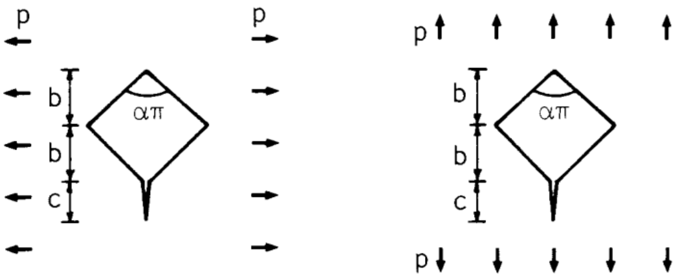

Figure 2.1: A Crack Emanating from a Corner of a Square Hole for Mode I Loading

Definition of geometry factor, *F* of Mode I Loading is as in Equation (3),

$$F_I = \frac{K_I}{P\sqrt{\left(\pi\left(b+\frac{c}{2}\right)\right)}} \tag{3}$$

The percentage of error is less than 1%.

2.4.2. Pure Shear Acting Along the Surface of the Square Hole (Mode II Loading)

Figure 2.4 below shows the geometry of a crack emanating from a corner of a square hole subject to Mode II loading [1].

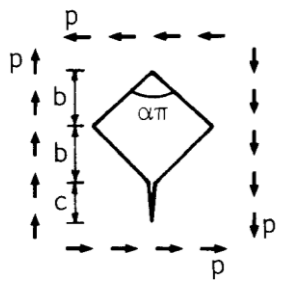

Figure 2.2: A Crack Emanating from a Corner of a Square Hole for Mode II Loading

Definition of geometry factor, *F* of Mode II Loading is as in Equation (4)

$$F_{II} = \frac{K_{II}}{P\sqrt{\left(\pi\left(b+\frac{c}{2}\right)\right)}} \tag{4}$$

The percentage of error is less than 1%.

All the solutions are determined for four variations of angles which are 30°, 60°, 90° and 120°. These angles will define the shape of the square hole. The models are also varied accordingly based on square length to the crack length ratio, *b/c* and vice versa, *c/b*.

2.5. KCALC Command in ANSYS

KCALC command is used to calculate the stress intensity factors associated with homogeneous isotropic linear elastic fracture mechanics assumptions. A displacement extrapolation method is used in the calculation. This method assumes that the displacement calculations are for the plane strain state. If the displacement calculations are performed using a plane stress formulation, the calculation of the stress intensity factors can be converted to the plane strain state. Other than that, the material's Poisson's ratio, crack face nodes and crack-tip coordinate system must be defined before performing KCALC command.

2.6. Plane 82 Mesh Element Option in ANSYS

PLANE82 is a higher order version of the 2-D, four-node element. It provides more accurate results for mixed (quadrilateral-triangular) automatic meshes and can tolerate irregular shapes without as much loss of accuracy [2]. The 8-node elements have compatible displacement shapes and are well suited to model curved boundaries. The 8-node element is defined by eight nodes having two degrees of freedom at each node: translations in the nodal *x* and *y* directions.

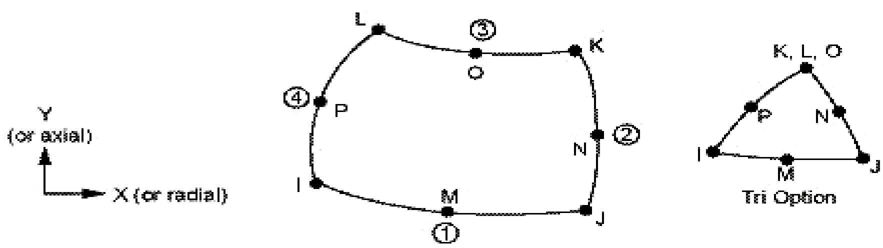

Figure 2.3: PLANE 82 Element Option

CHAPTER 3

METHODOLOGY

3.1. Research flow

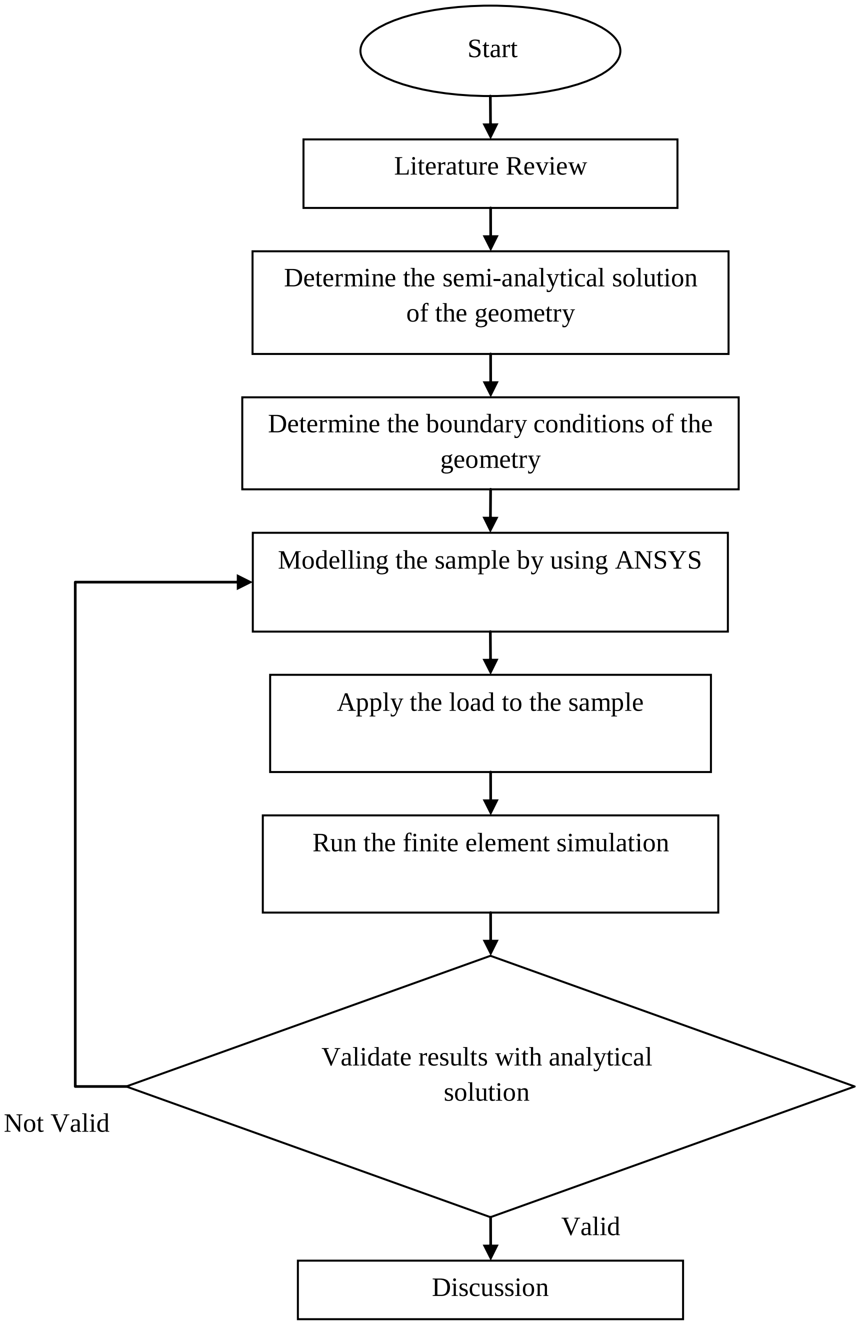

Figure 3.1: Research Methodology

3.2. Project Activities

The activities that have been done in order to complete this project are:

1. Determined the analytical solutions of stress intensity factor for all sets of geometries that are available in the literature.
2. Plotted graphs of geometry factor, *F* versus crack length to square length ratio, *c/b* and vice versa, *b/c* found for each geometry in the literature.
3. Modelled the cracks that are subjected to Mode I and Mode II loading for 30°, 60°, 90° and 120° variations of angle by using ANSYS and determined the stress intensity factor.
4. Computed the geometry factor, *F* for ANSYS results and compared the results obtained by ANSYS with the results from literature.

3.3. Modelling of a Crack Emanating from a Corner of a Square Hole in ANSYS

Throughout the project, ANSYS software was used to model and perform finite element analysis on all sets of crack geometries to determine the stress intensity factor. The material used was Stainless Steel Alloy 405 where the Young's Modulus, *E* is 200GPa and the Poisson's Ratio is 0.3. All models were assumed to be linear elastic and in plain strain condition. The elements properties selected for the models are as in Table 3.1.

Table 3.1: FEA Element Properties

Element Type	PLANE 82
Element Radius at the Crack Tip	*c*/8
No of elements around the crack tip	16
Mid-side node position	Skewed ¼ pt

The square length, *b* is set to be constant at 0.002m and there are four sets of square angles that need to be analyzed which are illustrated in Table 3.2 below.

Table 3.2: Ratios for Four Sets of Square Angles to be modelled

Square Angle	30°	60°	90°	120°
Crack length to square length ratio, *c/b*	0.0050	0.0048		
	0.0103	0.0100		
	0.0208	0.0200	0.0198	
	0.0497	0.0499	0.0504	0.0496
	0.1010	0.1000	0.1000	0.1010
	0.2000	0.2000	0.2000	0.2000
	0.3990	0.4000	0.4000	0.4030
	0.5950	0.6000	0.6010	0.6000
	0.7930	0.8000	0.8000	0.8000
	1.0000	1.0000	1.0000	1.0070
Square length to crack length ratio, *b/c*	0.8010	0.8000	0.8000	0.8050
	0.6070	0.6000	0.6000	0.6040
	0.4050	0.4000	0.4000	0.3990
	0.2030	0.2030	0.2000	0.2010

Three stages are involved in determining the stress intensity factor for crack geometries by using ANSYS. The stages and steps involved are shown below:

1. Pre-processor
   - Determine the type of element to be used.
   - Set the material model to be linear elastic and isotropic. Insert the values of Young's Modulus and Poisson's Ratio of the material.
   - Model the geometry by creating keypoints, lines and areas.
   - Define singular element on crack tip keypoint by using concentration keypoint.
   - Mesh the geometry.
   - Apply boundary conditions and pressure/ force to the model.

2. Solver
   - Define analysis type as static.
   - Solve the geometry.

3. Post-processor
   - Define crack path operation.
   - Create local coordinate system at the crack tip.
   - Calculate the stress intensity factor by using nodal calculation.

3.4. Modelling of a Crack Emanating From a Corner of a Square Hole for Mode I Loading

The geometry of interest is shown in Figure 2.3 in literature (Chapter 2). Due to the symmetric condition and for the ease of modelling, only a half of the geometry is modelled and analysed and the load applied to the model is 100MPa.

3.4.1. Uniform Tension in *x*-axis

Figure 3.2 below shows the half model of crack for Mode I loading of uniform tension in *x*-axis that is modelled by ANSYS where *c* is the crack length, σ is the applied load and *b* is the square length.

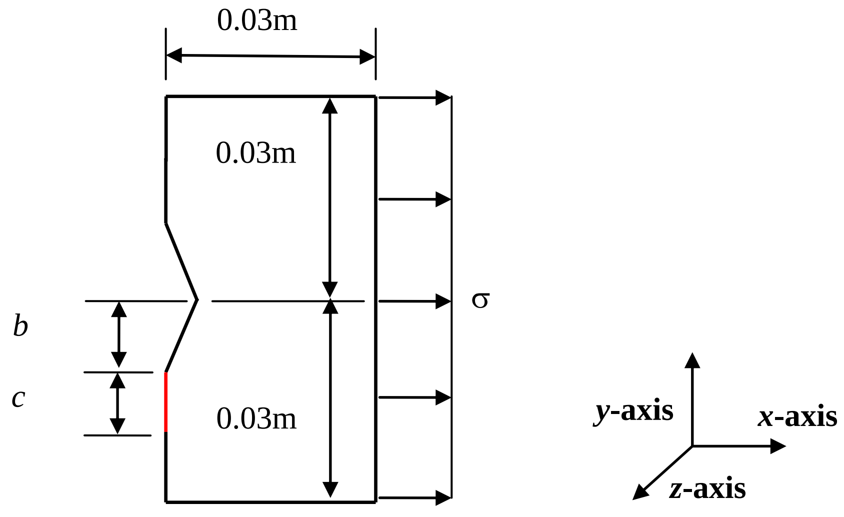

Figure 3.2: Half Model of Crack Geometry in ANSYS with Load Applied in *x*-axis

The steps to model and analyze the geometry are as follows:

1. Preprocessor
   - Give Jobname for the analysis.
   - Define element type.
   - Define material properties.
   - Model half of the geometry by creating keypoints, lines and areas
   - Assign the Concentration keypoint at the crack tip and mesh the area.
   - Apply symmetry boundary condition at the symmetrical lines. Do not apply any boundary condition on the crack line.
   - Apply negative pressure load on the right line of the geometry.

2. Solver
   - Set the analysis as static analysis.
   - Solve the problem.

3. Post-processor
   - Define crack path operation.
   - Create local coordinate system at the crack tip.
   - Perform KCALC command to find K_I value.

Figure 3.3 shows the ANSYS model for Mode I loading of uniform tension in *x*-axis for a crack emanating from a corner of a square hole.

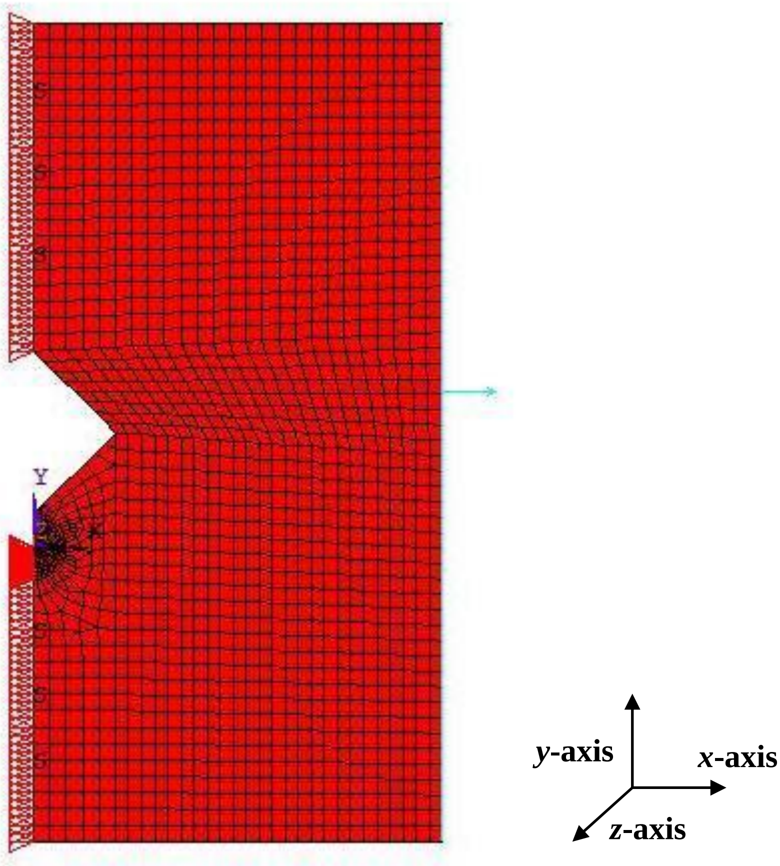

Figure 3.3: ANSYS Model for Mode I Loading of Uniform Tension in *x*-axis

3.4.2. Uniform Tension in *y*-axis

Figure 3.4 below shows the half model of crack for Mode I loading of uniform tension in *y*-axis that is modelled by ANSYS where *c* is the crack length, σ is the applied load and *b* is the square length.

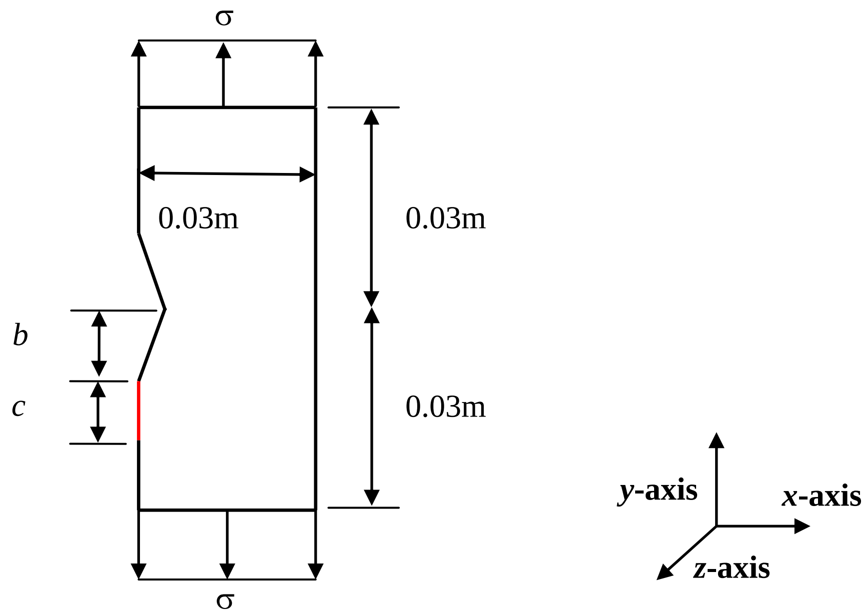

Figure 3.4: Half Model of Crack Geometry in ANSYS with Load Applied in *y*-axis

The steps to model and analyze the geometry are as follows:

1. Preprocessor
   - Give Jobname for the analysis.
   - Define element type.
   - Define material properties.
   - Model half of the geometry by creating keypoints, lines and areas
   - Assign the Concentration keypoint at the crack tip and mesh the area.
   - Apply symmetry boundary condition at the symmetrical lines. Do not apply any boundary condition on the crack line.
   - Apply negative pressure load on the top and bottom line of the geometry.

2. Solver
    - Set the analysis as static analysis.
    - Solve the problem.

3. Post-processor
    - Define crack path operation.
    - Create local coordinate system at the crack tip.
    - Perform KCALC command to find K_I value.

Figure 3.5 below shows the ANSYS model for Mode I loading of uniform tension in *y*-axis for a crack emanating from a corner of a square hole.

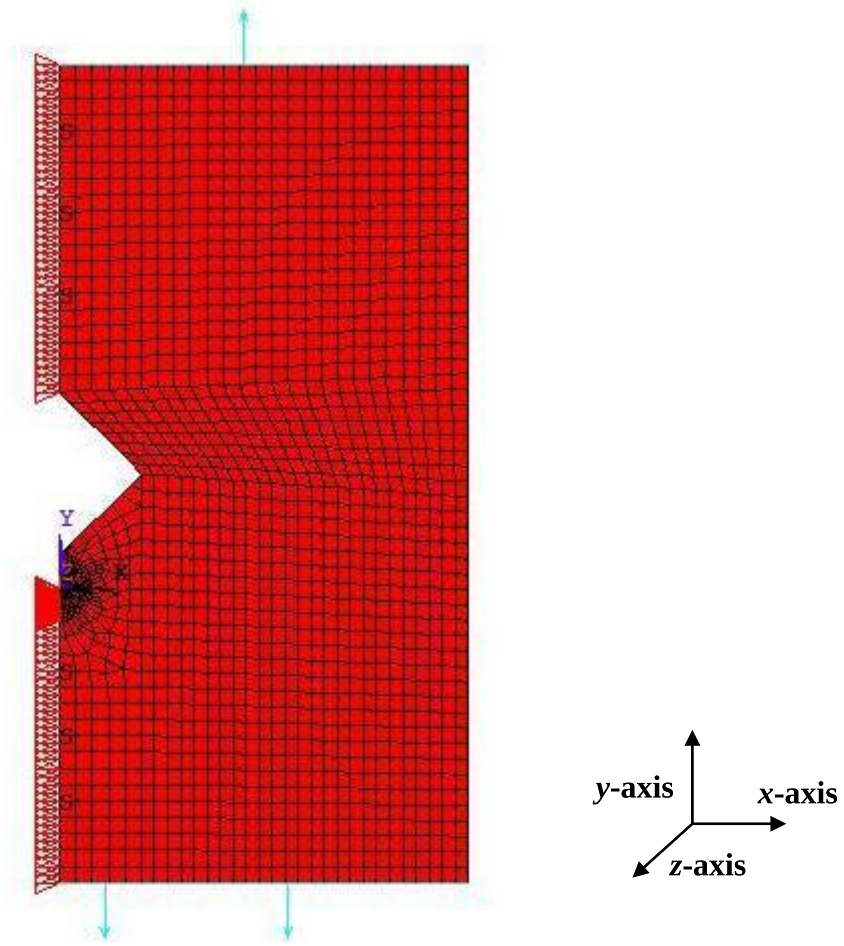

Figure 3.5: ANSYS Model for Mode I Loading of Uniform Tension in *y*-axis

3.5. Modelling of a Crack Emanating From a Corner of a Square Hole for Mode II Loading

The geometry of interest is shown in Figure 2.4 in the literature (Chapter 2). For pure shear acting along the model geometry, symmetric boundary condition is not applied. Instead of that, full body crack model is developed. In order to simulate the shear force, the equivalent force to stress of 100MPa is applied to each node on the surface of the geometry. Figure 3.6 below shows the full model of cracked-geometry that is modelled by ANSYS where *c* is the crack length, *P* is the applied force on each node at geometry surface and *b* is the square length.

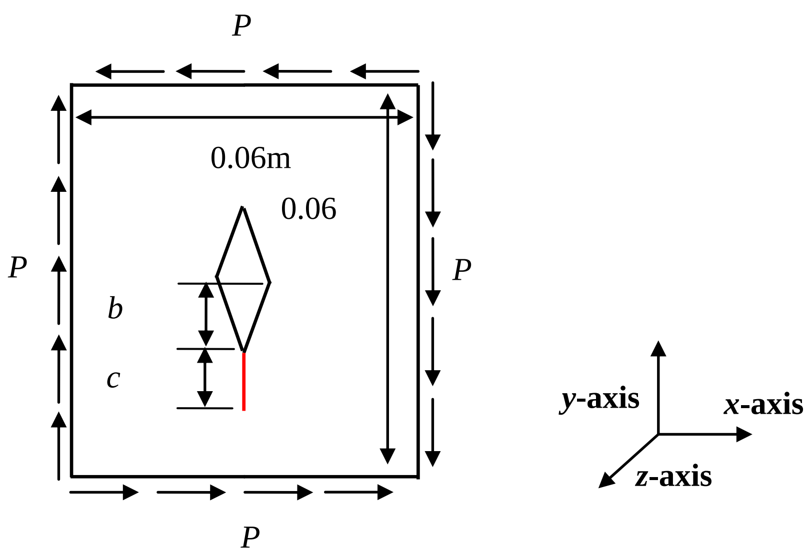

Figure 3.6: Full Model of Cracked-Geometry in ANSYS with Pure Shear Acting along the Geometry Surface

The steps to model and analyze the geometry are as follows:

1. Preprocessor
   - Give Jobname for the analysis.
   - Define element type.
   - Define material properties.
   - Model half of the geometry by creating keypoints, lines and areas
   - Assign the Concentration keypoint at the crack tip and mesh the area.
   - Reflect the meshing area at *y-z* plane to make complete crack model and merge all the nodes except the nodes along the crack length.
   - Apply equivalent force to stress of 100MPa on all nodes at the surface of the geometry.

2. Solver
   - Set the analysis as static analysis.
   - Solve the problem.

3. Post-processor
   - Define crack path operation.
   - Create local coordinate system at the crack tip.
   - Perform KCALC command to find K_{II} value.

Figure 3.7 shows the ANSYS model for Mode II loading for a crack emanating from a corner of a square hole.

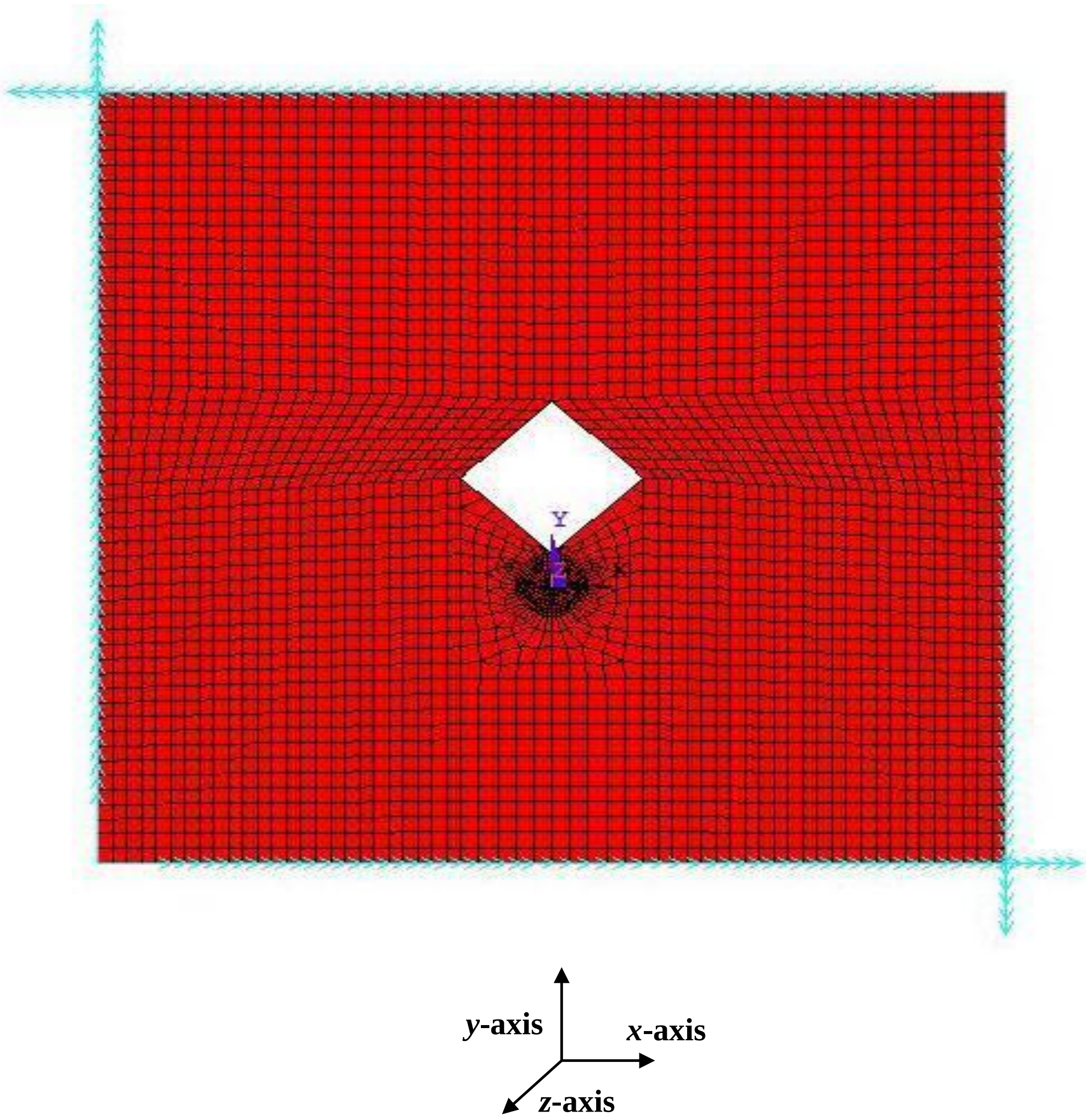

Figure 3.7: ANSYS Model for Mode II Loading

3.6. Gantt chart

Table 3.3: Gantt Chart for Final Year Project I

No	Detail/Week	1	2	3	4	5	6	7		8	9	10	11	12	13	14
1	Selection of Project Topic															
2	Preliminary research - Problem Identifying, Objective, Literature Review and Methodology															
3	Submission of Preliminary Report															
4	Project Work - Determine & Understand Analytical Solution															
6	Submission of Progress Report/Seminar															
7	Project Work - Determine Boundary Condition and Familiarization with ANSYS															
8	Submission of Interim Report Final Draft															
9	Oral presentation									Study Week						

Table 3.4: Gantt Chart for Final Year Project II

No	Detail/Week	1	2	3	4	5	6	7		8	9	10	11	12	13	14
1	Project Work – Mode I Loading Model Improvement	■	■	■	■											
2	Submission of Progress Report 1					●										
3	Project Work – Mode II Loading Analysis In ANSYS					■	■	■	■	■	■	■				
4	Submission of Progress Report 2									●						
6	Seminar									●						
7	Poster Exhibition											●				
8	Submission of Dissertation Final Draft															●
9	Oral presentation									Study Week						
10	Submission of Dissertation (Hard Bound)									After Oral Presentation						

CHAPTER 4
RESULTS AND DISCUSSIONS

4.1. Results of the Modelling of a Crack Emanating from a Corner of a Square Hole For Mode I Loading

The geometry of a crack emanating from a corner of a square hole is illustrated in Figure 2.3 in the literature (Chapter 2). The results are found for Mode I loading with four variations of angle which are 30°, 60°, 90° and 120°

4.1.1. Results of crack analysis subject to uniform tension in *x*-axis

Appendix 1 summarize the results for 30°, 60°, 90° and 120° cracked-holes subject to uniform tension in *x*-axis. The results are plotted in Figure 4.1.

Square Angle 30°

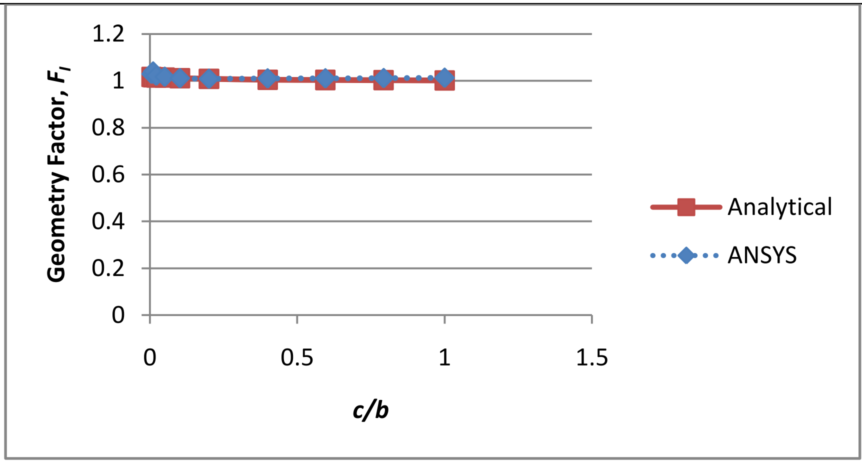

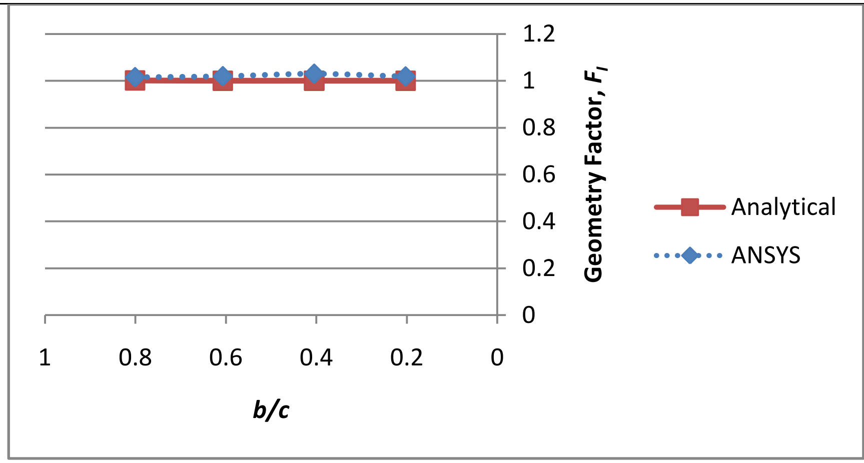

Square Angle 60°

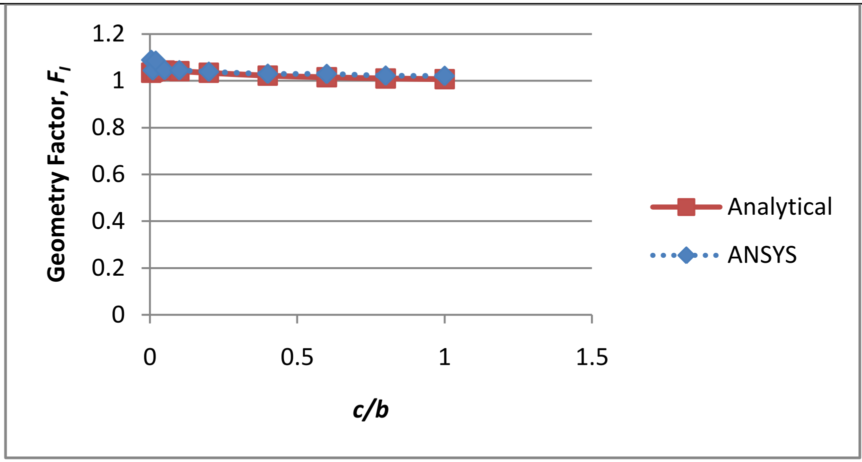

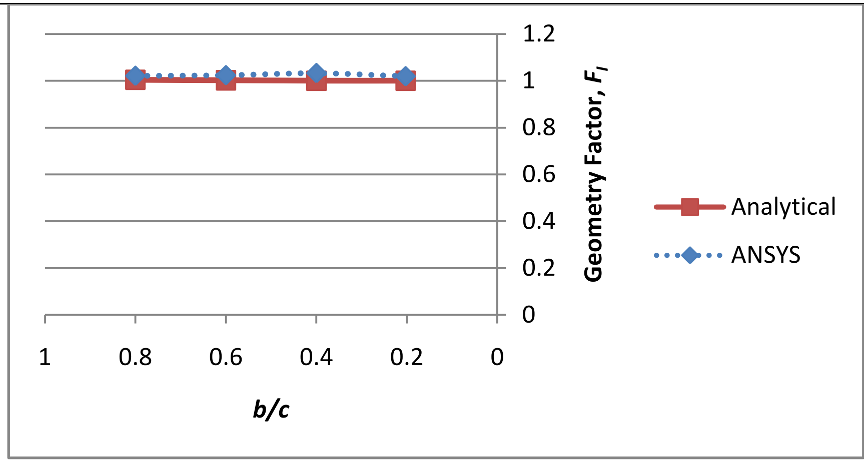

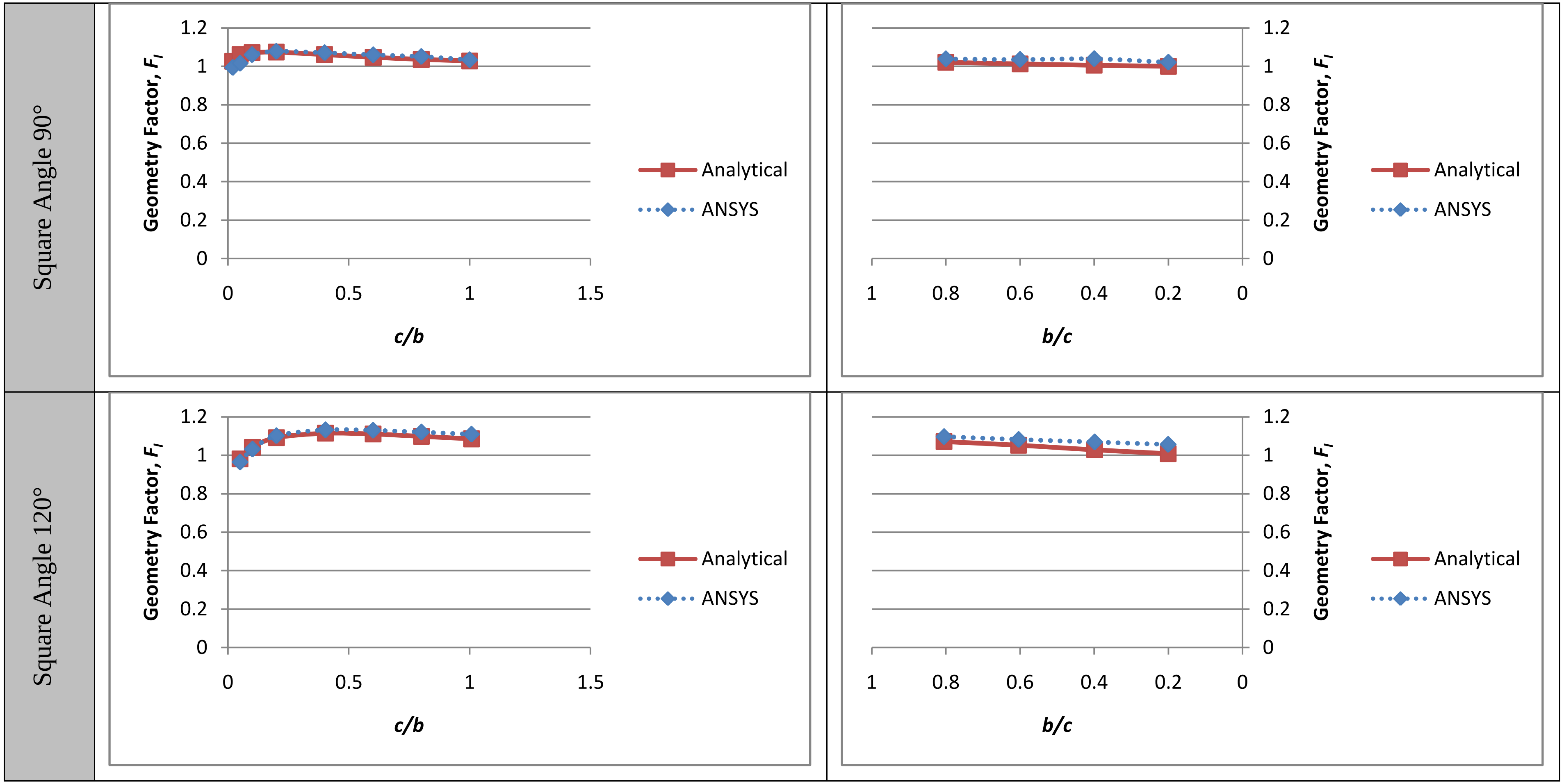

Figure 4.1: Graphical Comparisons of Results for Mode I Loading of Uniform Tension in *x*-axis

4.1.2. Discussions of Crack Analysis subject to Uniform Tension in *x*-axis

Figure 4.1 shows the results comparison between the geometry factors, *F* of ANSYS and the semi-analytical solution obtained from literature. Based on the results obtained for all the square angles, the graph between ANSYS and analytical solution has the same curved-line pattern. This indicates the results obtained by ANSYS are almost similar to the result found in semi-analytical solution.

According to the graph, in general the geometry factor, *F* will decrease as the crack length to square length ratio, *c/b* increases and square length to crack length ratio, *b/c* decreases. This relation shows that, as the crack length, *c* is increasing, the geometry factor, *F* will decrease. However, for square angle 90°, the geometry factor, *F* will increase from crack length to square length ratio, *c/b* of 0.0198 until 0.2 and decrease from crack length to square length ratio, *c/b* of 0.2 until 1. For square angle 120°, the geometry factor, *F* will increase from crack length to square length ratio, *c/b* of 0.0496 until 0.403 and decrease from crack length to square length ratio, *c/b* of 0.403 until 1.007.

There is slightly higher value of error and fluctuating pattern of results is observed at square angle 30°, 60° and 90° (detailed location is stated in the comparisons between all square angles). This is due to the position of the cracks which are situated more towards the edge of the square hole and this shape is difficult to be meshed. The comparisons of the results for uniform tension in *x*-axis for all square angles are as follows:

1. Square angle 30°

The results have low percentage of error with maximum percentage of error is 3.01% (at square length to crack length ratio, *b/c* of 0.405). The slightly higher value of error and fluctuating pattern of results is observed for the first three crack length to square length ratios, *c/b* of 0.005, 0.0103 and 0.0208, obtained by ANSYS.

2. Square angle 60°

The results have low percentage of error with maximum percentage of error is 5.29% (at crack length to square length ratio, *c/b* of 0.0048). The slightly higher value of error and fluctuating pattern of results is observed for crack length to square length ratios, *c/b* of 0.0048 and 0.02, obtained by ANSYS.

3. Square angle 90°

The results have low percentage of error with maximum percentage of error is 4.35% (at crack length to square length ratio, *c/b* of 0.0504). The slightly higher value of error and fluctuating pattern of results is observed for crack length to square length ratios, *c/b* of 0.0198 and 0.0504, obtained by ANSYS.

4. Square angle 120°

The results have low percentage of error with maximum percentage of error is 4.80% (at square length to crack length ratio, *b/c* of 0.201).

4.1.3. Results of crack analysis subject to uniform tension in *y*-axis

Appendix 2 summarize the results for 30°, 60°, 90° and 120° cracked-holes subject to uniform tension in *y*-axis. The results are plotted in Figure 4.2.

Square Angle 30°

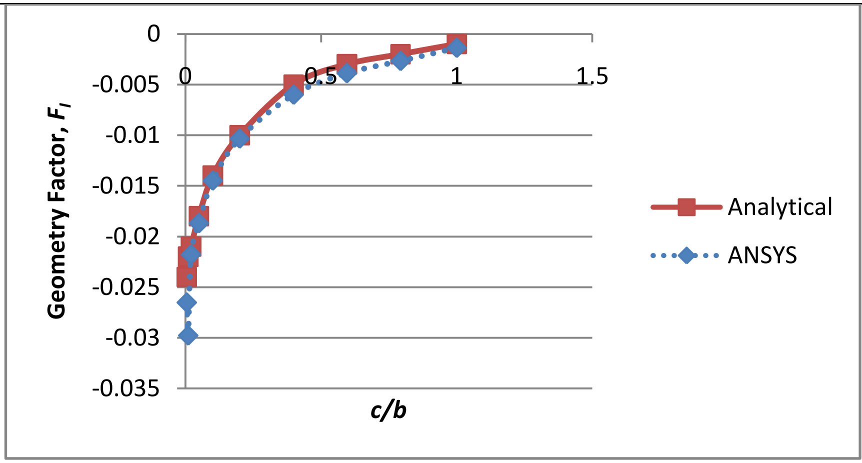

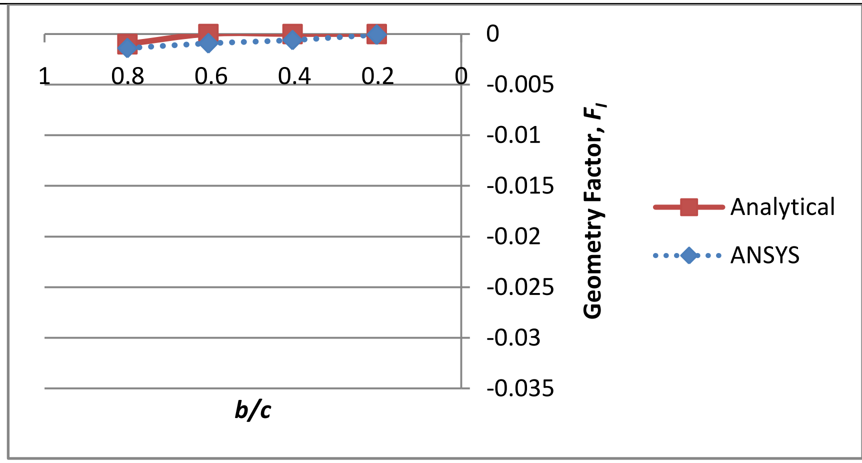

Square Angle 60°

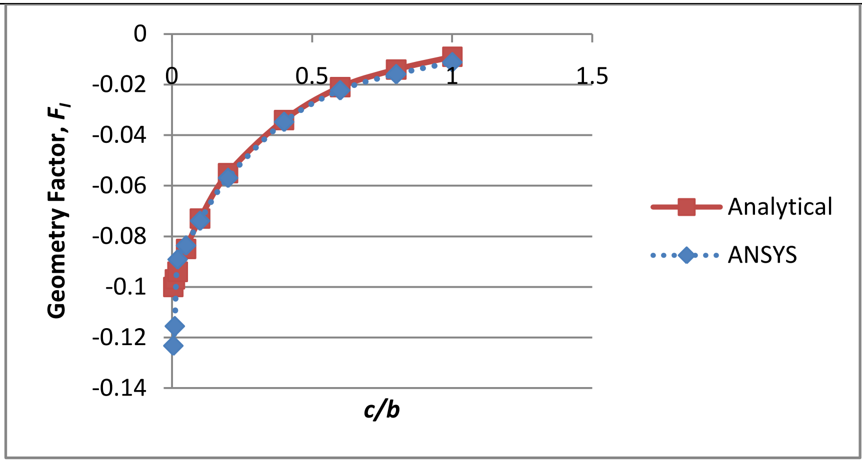

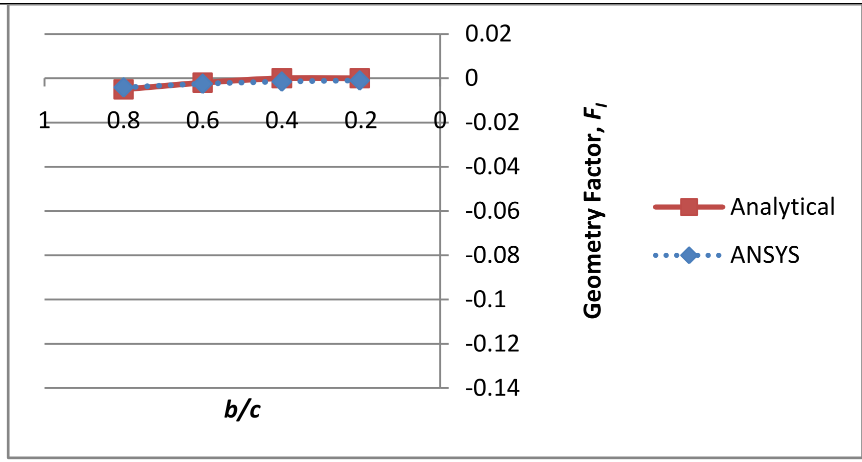

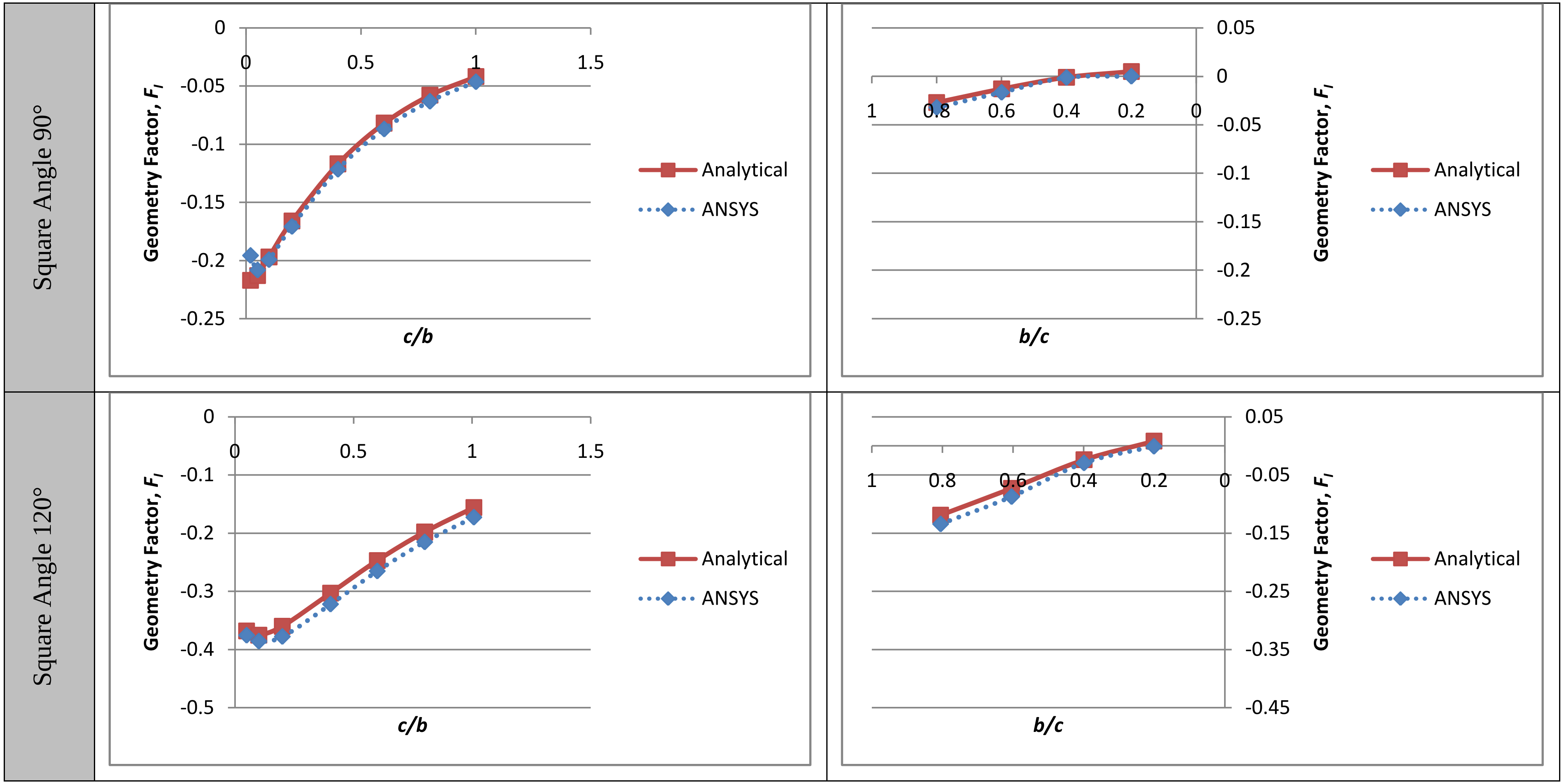

Figure 4.2: Graphical Comparisons of Results for Mode I Loading of Uniform Tension in *y*-axis

4.1.4. Discussions of Crack Analysis subject to Uniform Tension in *y*-axis

Figure 4.2 shows the results comparison between the geometry factors, *F* of ANSYS and the semi-analytical solution obtained from literature. Based on the results obtained for all the square angles, the graph between ANSYS and analytical solution has the same curved-line pattern. This indicates the results obtained by ANSYS are almost similar to the result found in semi-analytical solution.

According to the graph, in general the geometry factor, *F* will increase as the crack length to square length ratio, *c/b* increases and square length to crack length ratio, *b/c* decreases. This relation shows that, as the crack length, *c* is increasing, the geometry factor, *F* will increase. However, for square angle 120°, the geometry factor, *F* will decrease from crack length to square length ratio, *c/b* of 0.0496 until 0.101 and increase from crack length to square length ratio, *c/b* of 0.101 until 1.007.

There is slightly higher value of error and fluctuating pattern of results is observed in square angle 30°, 60°, 90° and 120° (detailed location is stated in the comparisons between all square angles). This is due to the position of the cracks which are situated more towards the edge of the square hole and this shape is difficult to be meshed.

The percentage of error for certain crack length to square length ratio, *c/b* and for square length to crack length ratio, *b/c* are very high compared to others for example at square angle 30°, 60°, 90° and 120° (detailed location is stated in the comparisons between all square angles). This is because of the semi-analytical solution value is too small (as it is approaching 0) and this gives higher value of error. However, in comparing the graph for ANSYS and semi-analytical solution geometry factor, *F*, the results is considered acceptable**.** The comparisons of the results for uniform tension in *y*-axis for all square angles are as follows:

1. Square angle 30°

The results have moderate percentage of error with maximum percentage of error of 40.23% (at square length to crack length ratio, *b/c* of 0.801). The slightly higher value of error and fluctuating pattern of results is observed for the crack length to square length ratios, *c/b* of 0.005 and 0.0103, obtained by ANSYS. The crack length to square length ratios, *c/b* of 0.793 and 1 and square length to crack length ratio, *b/c* of 0.801 have higher percentage of error compared to others.

2. Square angle 60°

The results have moderate percentage of error with maximum percentage of error of 25.94% (at square length to crack length ratio, *b/c* of 0.6). The slightly higher value of error and fluctuating pattern of results is observed for the first two crack length to square length ratio, *c/b* which are 0.0048 and 0.01, obtained by ANSYS. The crack length to square length ratio, *c/b* of 1 and square length to crack length ratios, *b/c* of 0.8 and 0.6 have higher percentage of error compared to others.

3. Square angle 90°

The results have moderate percentage of error with maximum percentage of error of 100.86%. The maximum percentage of error is observed at square length to crack length ratio, *b/c* of 0.2 where the ANSYS result indicates negative value of geometry factor, *F* while the semi-analytical solution result have positive value of geometry factor, *F*. The slightly higher value of error and fluctuating pattern of results is observed for the first three crack length to square length ratios, *c/b* of 0.0198, 0.0504 and 0.1, obtained by ANSYS. The square length to crack length ratio, *b/c* of 0.4 and 0.2 has higher percentage of error compared to others.

4. Square angle 120°

The results have moderate percentage of error with maximum percentage of error of 111.59%. This error is observed at square length to crack length ratio, *b/c* of 0.201 where the ANSYS results indicates negative value of geometry factor, *F* while the semi-analytical solution result have positive value of geometry factor, *F*. The crack length to square length ratio, *c/b* of 1.007 and square length to crack length ratios, *b/c* of 0.805, 0.604, 0.399 and 0.201 have higher percentage of error compared to others.

4.2. Results of the Modelling of a Crack Emanating From a Corner of a Square Hole for Mode II Loading

The geometry of a crack emanating from a corner of a square hole is illustrated in Figure 2.4 in literature review section. The results are found for Mode II loading with four variations of angle which are 30°, 60°, 90° and 120°. Appendix 3 summarize the results for 30°, 60°, 90° and 120° cracked-holes subject to Mode II loading. The results are plotted in Figure 4.3.

Square Angle 30°

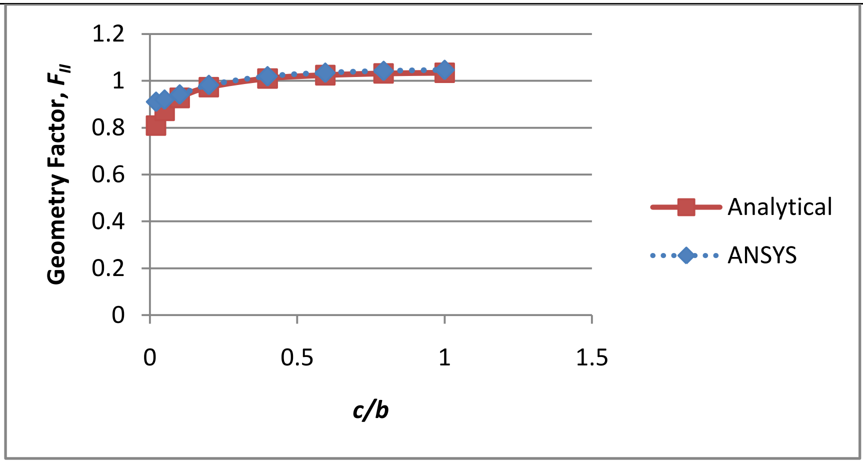

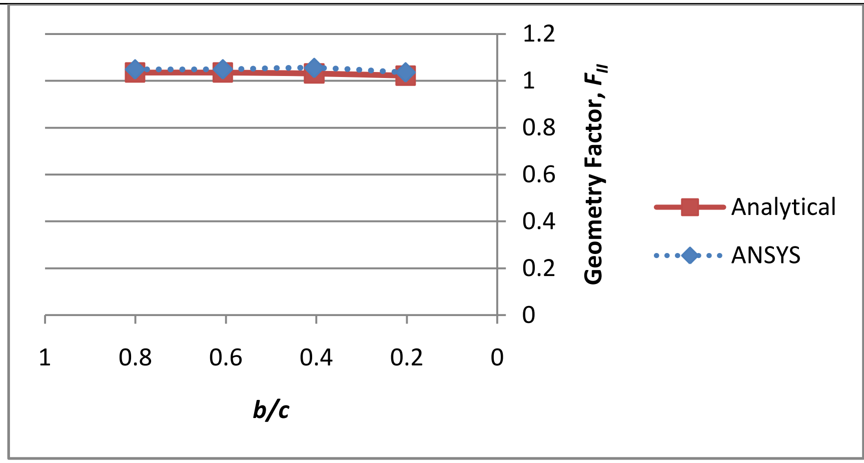

Square Angle 60°

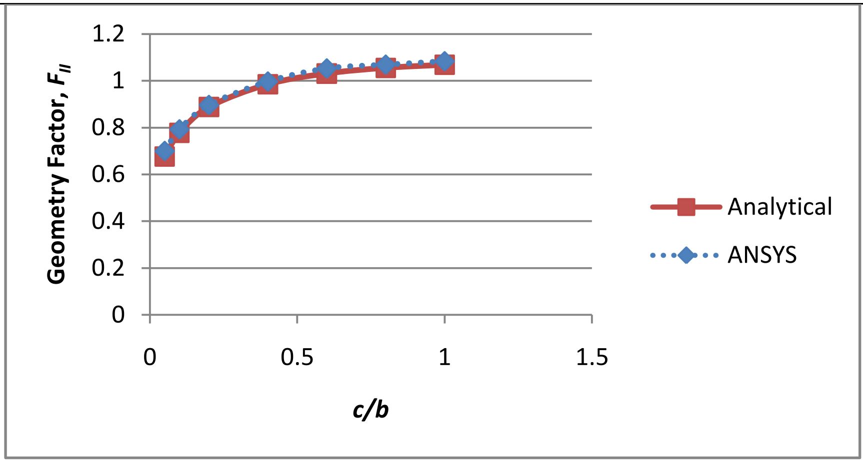

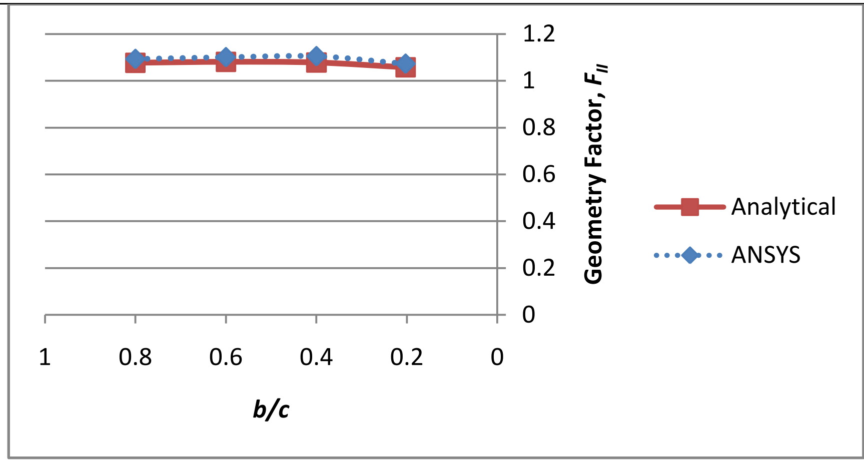

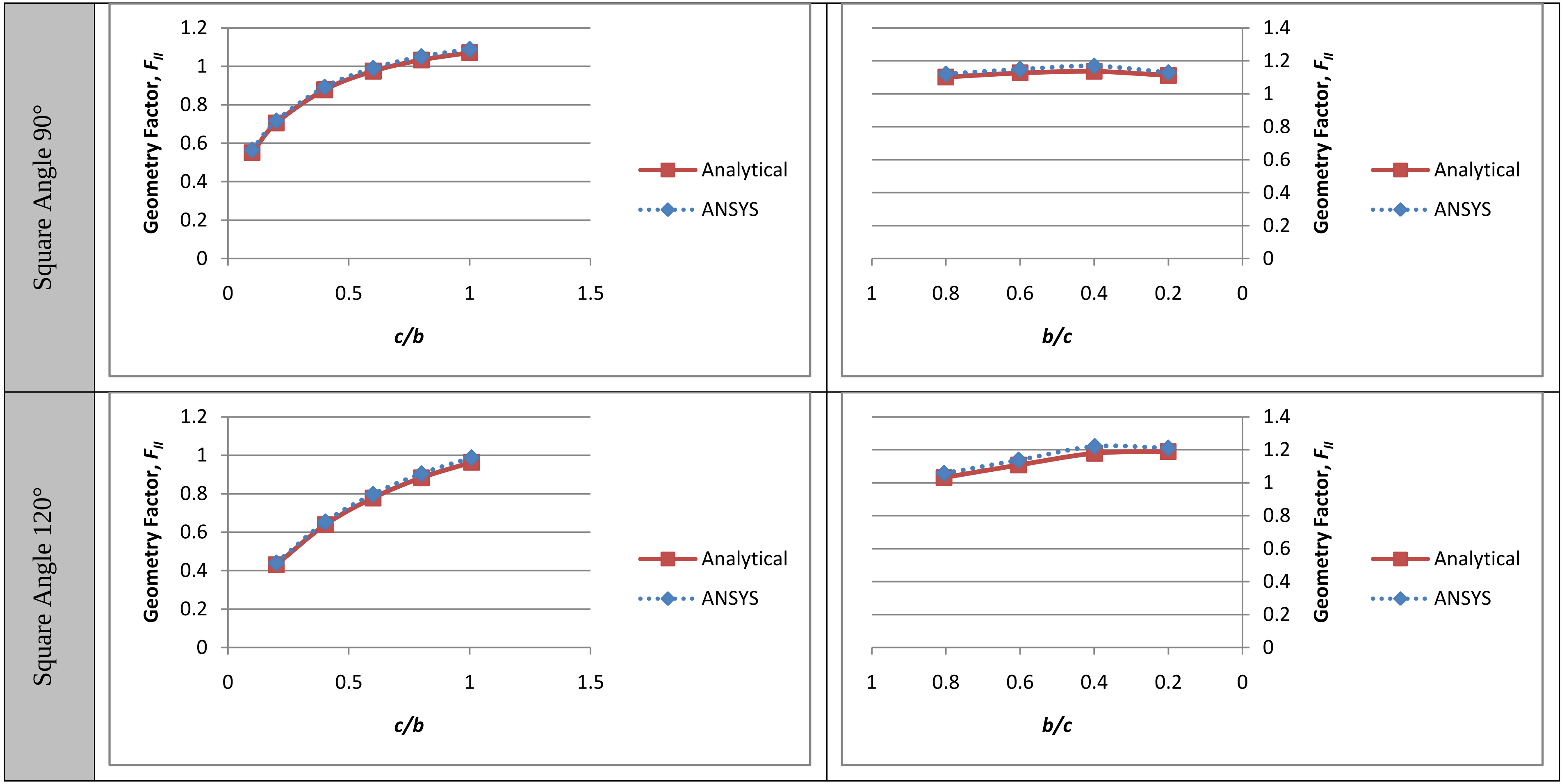

Figure 4.5: Graphical Comparisons of Results for Mode II Loading

4.2.1. Discussions of Crack Analysis for Mode II Loading

Figure 4.3 shows the results comparison between the geometry factors, *F* of ANSYS and the semi-analytical solution obtained from literature. Based on the results obtained for all the square angles, the graph between ANSYS and analytical solution has the same curved-line pattern. This indicates the results obtained by ANSYS are almost similar to the result found in semi-analytical solution.

According to the graph, geometry factor, *F* will increase as the crack length to square length ratio, *c/b* increases and square length to crack length ratio, *b/c* decreases. This relation shows that, as the crack length, *c* is increased, the geometry factor, *F* will increase. However, for square angle 30°, the geometry factor, *F* will increase from square length to crack length ratio, *b/c* of 0.801 until 0.607 and decrease from square length to crack length ratio, *b/c* of 0.607 until 0.203. For square angle 60°, the geometry factor, *F* will increase from square length to crack length ratio, *b/c* of 0.8 until 0.6 and decrease from square length to crack length ratio, *b/c* of 0.6 until 0.203. For square angle 90°, the geometry factor, *F* will increase from square length to crack length ratio, *b/c* of 0.8 until 0.4 and decrease from square length to crack length ratio, *b/c* of 0.4 until 0.2.

There is slightly higher value of error and fluctuating pattern of results observed in square angle 30° (detailed location is stated in the comparisons between all square angles). This is due to the position of the cracks which are situated more towards the edge of the square hole and this shape is difficult to be meshed. The comparisons of the results for uniform tension in *y*-axis for all square angles are as follows:

1. Square angle 30°

The results have low percentage of error with maximum percentage of error is 12.5% (at crack length to square length ratio, *c/b* of 0.0208). The slightly higher value of error and fluctuating pattern of results is observed for the first two crack length to square length ratios, *c/b* of 0.0208 and 0.0497, obtained by ANSYS.

2. Square angle 60°

The results has low percentage of error with maximum percentage of error is 3.40% (at crack length to square length ratio, *c/b* of 0.0499).

3. Square angle 90°

The results has low percentage of error with maximum percentage of error is 2.83% (at square length to crack length ratio, *b/c* of 0.4).

4. Square angle 120°

The results has low percentage of error with maximum percentage of error is 3.60% (at square length to crack length ratio, *b/c* of 0.399).

4.3. Comparison of Geometry Factor, *F* Results for Different Square Angles

Table 4.1, Table 4.2, Table 4.3, Figure 4.4, Figure 4.5 and Figure 4.6 illustrate the geometry factor, *F* results comparisons for four variations of square angle. The square angles considered are 30°, 60°, 90° and 120°. The geometry factor, *F* values selected is for crack length to square length ratio, *c/b* of 0.4 where it has low percentage of error.

4.3.1. Geometry Factor, *F* Results for Different Square-Angled-Cracked-Body Subject to Uniform Tension in *x*-axis

Table 4.1: Geometry Factor, *F* Results for Different Square-Angled-Cracked-Body Subject to Uniform Tension in *x*-axis

Crack length to Square length ratio, *c/b*	0.4	
Square Angle	ANSYS Geometry Factor, F_I	Analytical Geometry Factor, F_I
30°	1.0129	1.001
60°	1.0297	1.022
90°	1.0704	1.061
120°	1.1317	1.114

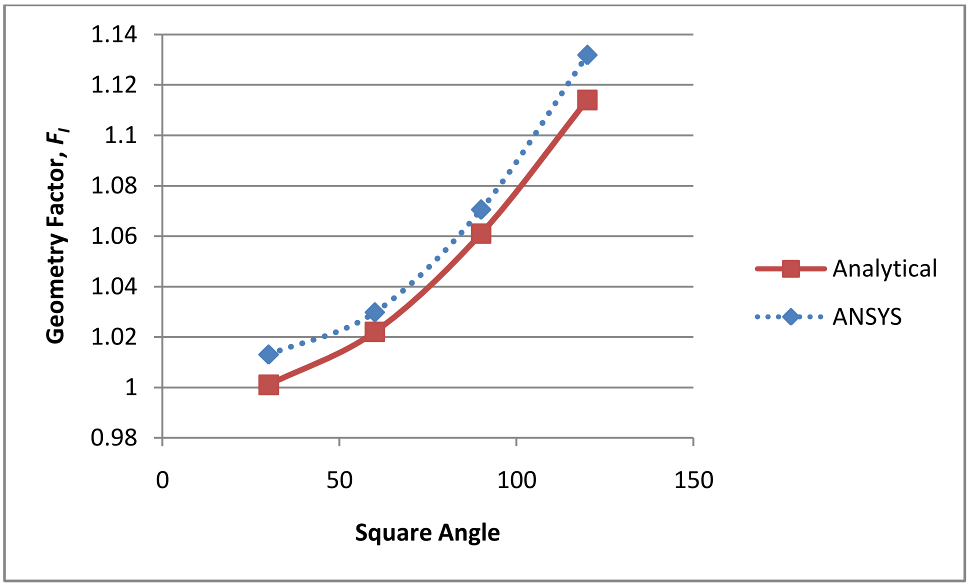

Figure 4.4: Variation of Geometry Factor, *F* with Square Angles (*x*-axis loading)

Based on the graph in Figure 4.4, it shows that as the square angle increases, the geometry factor, *F* will increase.

4.3.2. Geometry Factor, *F* Results for Different Square-Angled-Cracked-Body Subject to Uniform Tension in *y*-axis

Table 4.2: Geometry Factor, *F* Results for Different Square-Angled-Cracked-Body Subject to Uniform Tension in *y*-axis

Crack length to Square length ratio, *c/b*	0.4	
Square Angle	ANSYS Geometry Factor, F_I	Analytical Geometry Factor, F_I
30°	-0.0060	-0.005
60°	-0.0347	-0.034
90°	-0.1216	-0.117
120°	-0.3221	-0.303

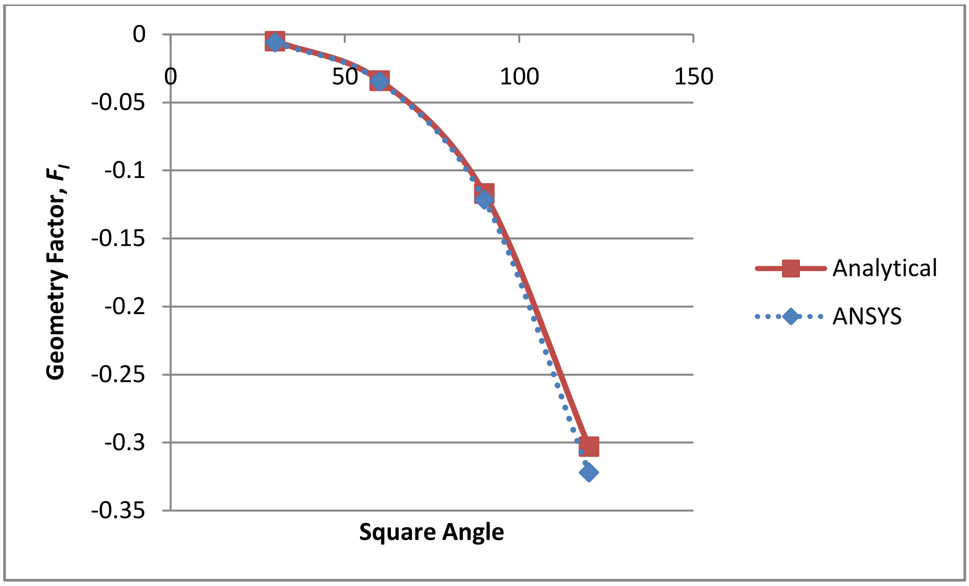

Figure 4.5: Variation of Geometry Factor, *F* with Square Angles (*y*-axis loading)

Based on the graph in Figure 4.5, it shows that as the square angle increases, the geometry factor, *F* will increase (in magnitude).

4.3.3. Geometry Factor, *F* Results for Different Square-Angled-Cracked-Body Subject to Mode II Loading

Table 4.3**:** Geometry Factor, F Results for Different Square-Angled-Cracked-Body Subject to Mode II Loading

Crack length to Square length ratio, *c/b*	0.4	
Square Angle	ANSYS Geometry Factor, F_I	Analytical Geometry Factor, F_I
30°	1.018	1.01
60°	0.996	0.985
90°	0.891	0.878
120°	0.653	0.639

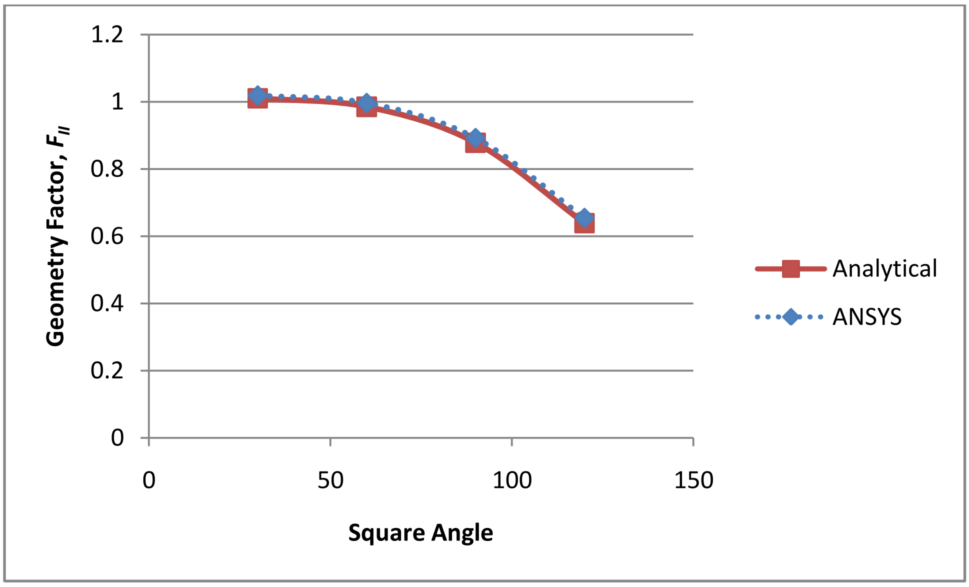

Figure 4.6: Variation of Geometry Factor, *F* with Square Angles for Mode II Loading

Based on the graph in Figure 4.6, it shows that as the square angle increases, the geometry factor, *F* will decrease.

CONCLUSIONS

In conclusion, the objectives of the project to model and determine the stress intensity factor for a crack emanating from a corner of a square hole by using ANSYS and compare the results with those results obtained semi-analytically is fully achieved. In this project, the model is subjected to 2 mode of loading which are Mode I (uniform tension in x and y-axis) and Mode II loading (pure shear acting along the surface of the square hole model).

For Mode I loading (uniform tension in x-axis), it can be concluded that as the crack length, c is increased, the geometry factor, F will decrease. In comparing the geometry factor, F for different values of square angle, the results concludes that as the square angle is increased, the geometry factor, F will increase.

For Mode I loading (uniform tension in y-axis), it can be concluded that as the crack length, c is increase, the geometry factor, F will increase. In comparing the geometry factor, F for different values of square angle, the results concludes that as the square angle is increased, the geometry factor, F will increase.

For Mode II loading, it can be concluded that as the crack length, c is increase, the geometry factor, F will increase. In comparing the geometry factor, F for different values of square angle, the results concludes that as the square angle is increased, the geometry factor, F will decrease.

The accuracy of this work is expressed in term of percentage of error between the results obtained by using ANSYS with the one found in the literature. For Mode I uniform tension in x-axis loading crack configurations, maximum percentage of error is 5.30% (square angle 60°). For Mode I uniform tension in y-axis loading crack configurations, maximum percentage of error is 111.59% (square angle 120°). For Mode II loading crack configurations, maximum percentage of error is 12.5% (square angle 30°). The accuracy of the project is dependent on many factors such as the crack configuration, ANSYS environment and also meshing of the model.

REFERENCES

1. Y. Murakami, *Stress Intensity Factors Handbook*, Pergamon Press, New York (1987)
2. ANSYS Inc *Theory Reference* (2009)
3. L. P. Pook, *Linear Elastic Fracture Mechanics for Engineers: Theory and Application*, WIT Press, (2000)
4. M. Janssen, J. Zuidema, R. Wanhill, *Fracture Mechanics 2nd Edition*, Spon Press, (2004)
5. Walter D. Pilkey, *Formulas for Stress, Strain and Structural Matrices* (2001)
6. Dr. A.-V. Phan, *ANSYS Tutorial 2-D Fracture Analysis*, University of South Alabama (2001)
7. *http://www.efunda.com/formulae/solid_mechanics/fracture_mechanics/fm_lefm.cfm*

Appendix 1: ANSYS Results for Mode I Loading of Uniform Tension in *x*-axis

Square Angle	30°			Square Angle	60°		
Crack length to Square length ratio, *c/b*	ANSYS Geometry Factor, F_I	Analytical Geometry Factor, F_I	Error (%)	Crack length to Square length ratio, *c/b*	ANSYS Geometry Factor, F_I	Analytical Geometry Factor, F_I	Error (%)
0.005	1.0291	1.016	1.29	0.0048	1.0888	1.034	5.29
0.0103	1.0396	1.015	2.42	0.01	1.0441	1.038	0.58
0.0208	1.0215	1.014	0.74	0.02	1.0853	1.041	4.25
0.0497	1.0171	1.013	0.40	0.0499	1.0452	1.044	0.11
0.101	1.0112	1.011	0.02	0.1	1.0447	1.041	0.35
0.2	1.0087	1.008	0.07	0.2	1.0382	1.034	0.40
0.399	1.0103	1.004	0.62	0.4	1.0297	1.022	0.75
0.595	1.0105	1.003	0.75	0.6	1.0289	1.015	1.36
0.793	1.0114	1.002	0.94	0.8	1.0218	1.010	1.16
1	1.0129	1.001	1.19	1	1.0207	1.007	1.36
Square length to crack length ratio, *b/c*	ANSYS Geometry Factor, F_I	Analytical Geometry Factor, F_I	Error (%)	Square length to crack length ratio, *b/c*	ANSYS Geometry Factor, F_I	Analytical Geometry Factor, F_I	Error (%)
0.801	1.0154	1.001	1.44	0.8	1.0207	1.004	1.66
0.607	1.0195	1	1.95	0.6	1.0233	1.002	2.13
0.405	1.0301	1	3.01	0.4	1.0325	1	3.25
0.203	1.0185	1	1.85	0.203	1.0189	1	1.89
Average			1.19	Average			1.75

Square Angle	90°			Square Angle	120°		
Crack length to Square length ratio, c/b	ANSYS Geometry Factor, F_I	Analytical Geometry Factor, F_I	Error (%)	Crack length to Square length ratio, c/b	ANSYS Geometry Factor, F_I	Analytical Geometry Factor, F_I	Error (%)
0.0198	0.9937	1.026	3.14				
0.0504	1.0157	1.062	4.35	0.0496	0.9649	0.981	1.63
0.1	1.0602	1.071	1.00	0.101	1.0317	1.041	0.89
0.2	1.0774	1.074	0.32	0.2	1.1012	1.091	0.93
0.4	1.0704	1.061	0.88	0.403	1.1317	1.114	1.59
0.601	1.0594	1.047	1.18	0.6	1.1294	1.11	1.75
0.8	1.0506	1.036	1.41	0.8	1.1202	1.098	2.02
1	1.0338	1.028	0.56	1.007	1.1092	1.085	2.23
Square length to crack length ratio, b/c	ANSYS Geometry Factor, F_I	Analytical Geometry Factor, F_I	Error (%)	Square length to crack length ratio, b/c	ANSYS Geometry Factor, F_I	Analytical Geometry Factor, F_I	Error (%)
0.8	1.0381	1.02	1.77	0.805	1.0963	1.071	2.37
0.6	1.0348	1.012	2.26	0.604	1.0816	1.052	2.81
0.4	1.0387	1.005	3.35	0.399	1.0689	1.028	3.98
0.2	1.0205	1	2.05	0.201	1.0564	1.008	4.80
Average			0.44	Average			1.81

Appendix 2: ANSYS Results for Mode I Loading of Uniform Tension in *y*-axis

Square Angle	30°			Square Angle	60°		
Crack length to Square length ratio, *c/b*	ANSYS Geometry Factor, F_I	Analytical Geometry Factor, F_I	Error (%)	Crack length to Square length ratio, *c/b*	ANSYS Geometry Factor, F_I	Analytical Geometry Factor, F_I	Error (%)
0.005	-0.0265	-0.024	10.49	0.0048	-0.1232	-0.1	23.21
0.0103	-0.0297	-0.022	35.33	0.01	-0.1154	-0.097	19.06
0.0208	-0.0217	-0.021	3.738	0.02	-0.0891	-0.094	5.191
0.0497	-0.0187	-0.018	3.862	0.0499	-0.0836	-0.085	1.632
0.101	-0.0144	-0.014	3.465	0.1	-0.0738	-0.073	1.156
0.2	-0.0103	-0.01	3.405	0.2	-0.0568	-0.055	3.414
0.399	-0.0060	-0.005	20.27	0.4	-0.0347	-0.034	2.185
0.595	-0.0039	-0.003	29.84	0.6	-0.0222	-0.021	6.050
0.793	-0.0026	-0.002	34.35	0.8	-0.0158	-0.014	13.38
1	-0.00139	-0.001	38.91	1	-0.0111	-0.009	23.96
Square length to crack length ratio, *b/c*	ANSYS Geometry Factor, F_I	Analytical Geometry Factor, F_I	Error (%)	Square length to crack length ratio, *b/c*	ANSYS Geometry Factor, F_I	Analytical Geometry Factor, F_I	Error (%)
0.801	-0.0014	-0.001	40.23	0.8	-0.00414	-0.005	17.10
0.607	-0.00095	0	N/A	0.6	-0.00252	-0.002	25.94
0.405	-0.00062	0	N/A	0.4	-0.00154	0	N/A
0.203	-8.6E-05	0	N/A	0.203	-0.00104	0	N/A
Average			25.31	Average			14.23

Square Angle	90°			Square Angle	120°		
Crack length to Square length ratio, *c/b*	ANSYS Geometry Factor, F_I	Analytical Geometry Factor, F_I	Error (%)	Crack length to Square length ratio, *c/b*	ANSYS Geometry Factor, F_I	Analytical Geometry Factor, F_I	Error (%)
0.0198	-0.1956	-0.217	9.84				
0.0504	-0.2081	-0.213	2.28	0.0496	-0.3756	-0.368	2.09
0.1	-0.1993	-0.197	1.16	0.101	-0.3857	-0.375	2.87
0.2	-0.1707	-0.166	2.85	0.2	-0.3778	-0.36	4.95
0.4	-0.1216	-0.117	3.93	0.403	-0.3221	-0.303	6.31
0.601	-0.0869	-0.082	6.09	0.6	-0.2652	-0.247	7.36
0.8	-0.0631	-0.058	8.93	0.8	-0.2152	-0.198	8.68
1	-0.0463	-0.042	10.37	1.007	-0.1727	-0.156	10.70
Square length to crack length ratio, *b/c*	ANSYS Geometry Factor, F_I	Analytical Geometry Factor, F_I	Error (%)	Square length to crack length ratio, *b/c*	ANSYS Geometry Factor, F_I	Analytical Geometry Factor, F_I	Error (%)
0.8	-0.0321	-0.027	19.14	0.805	-0.1344	-0.119	12.94
0.6	-0.0166	-0.013	27.74	0.604	-0.0874	-0.073	19.77
0.4	-0.0013	-0.001	31.32	0.399	-0.0295	-0.024	23.06
0.2	-4.311E-05	0.005	100.8	0.201	-0.0009	0.008	111.5
Average			39.96	Average			2.02

Appendix 3: ANSYS Results for Mode II Loading

Square Angle	30°			Square Angle	60°		
Crack length to Square length ratio, *c/b*	ANSYS Geometry Factor, F_{II}	Analytical Geometry Factor, F_{II}	Error (%)	Crack length to Square length ratio, *c/b*	ANSYS Geometry Factor, F_{II}	Analytical Geometry Factor, F_{II}	Error (%)
0.0208	0.9101	0.809	12.5				
0.0497	0.9193	0.872	5.43	0.0499	0.7000	0.677	3.40
0.101	0.9411	0.927	1.53	0.1	0.7923	0.778	1.84
0.2	0.9817	0.973	0.89	0.2	0.8962	0.888	0.92
0.399	1.0187	1.01	0.86	0.4	0.9962	0.985	1.14
0.595	1.0338	1.024	0.95	0.6	1.0519	1.031	2.02
0.793	1.0414	1.031	1.01	0.8	1.0681	1.055	1.24
1	1.0457	1.034	1.13	1	1.0826	1.068	1.36
Square length to crack length ratio, *b/c*	ANSYS Geometry Factor, F_{II}	Analytical Geometry Factor, F_{II}	Error (%)	Square length to crack length ratio, *b/c*	ANSYS Geometry Factor, F_{II}	Analytical Geometry Factor, F_{II}	Error (%)
0.801	1.0485	1.035	1.30	0.8	1.0930	1.077	1.48
0.607	1.0488	1.035	1.33	0.6	1.1005	1.081	1.81
0.405	1.0546	1.031	2.28	0.4	1.1047	1.078	2.47
0.203	1.0358	1.022	1.35	0.203	1.0727	1.057	1.48
Average			2.55	Average			1.74

Square Angle	90°			Square Angle	120°		
Crack length to Square length ratio, *c/b*	ANSYS Geometry Factor, F_{II}	Analytical Geometry Factor, F_{II}	Error (%)	Crack length to Square length ratio, *c/b*	ANSYS Geometry Factor, F_{II}	Analytical Geometry Factor, F_{II}	Error (%)
0.1	0.5645	0.551	2.45				
0.2	0.7157	0.705	1.52	0.2	0.4403	0.431	2.18
0.4	0.8917	0.878	1.56	0.403	0.6537	0.639	2.31
0.601	0.9902	0.975	1.56	0.6	0.7968	0.778	2.42
0.8	1.0506	1.033	1.70	0.8	0.9043	0.883	2.41
1	1.0888	1.071	1.66	1.007	0.9875	0.963	2.54
Square length to crack length ratio, *b/c*	ANSYS Geometry Factor, F_{II}	Analytical Geometry Factor, F_{II}	Error (%)	Square length to crack length ratio, *b/c*	ANSYS Geometry Factor, F_{II}	Analytical Geometry Factor, F_{II}	Error (%)
0.8	1.1203	1.101	1.75	0.805	1.0567	1.031	2.49
0.6	1.1486	1.126	2.01	0.604	1.1376	1.107	2.76
0.4	1.1682	1.136	2.83	0.399	1.2204	1.178	3.60
0.2	1.1284	1.111	1.56	0.201	1.2108	1.189	1.84
Average			1.86	Average			2.51